The Plant Cell, Vol. 17, 537–547, February 2005, www.plantcell.org © 2005 American Society of Plant Biologists

The Arabidopsis WAVY GROWTH 2 Protein Modulates Root Bending in Response to Environmental Stimuli

Susumu Mochizuki,[a,1] Akiko Harada,[a,1,2] Sayaka Inada,[a] Keiko Sugimoto-Shirasu,[b] Nicola Stacey,[b] Takuji Wada,[c,3] Sumie Ishiguro,[c,4] Kiyotaka Okada,[a,c] and Tatsuya Sakai[a,5]

[a] RIKEN Plant Science Center, Tsurumi-ku, Yokohama, Kanagawa 230-0045, Japan
[b] Department of Cell and Developmental Biology, John Innes Centre, Norwich, NR4 7UH, United Kingdom
[c] Department of Botany, Graduate School of Science, Kyoto University, Kitashirakawa-Oiwake-cho, Sakyo-ku, Kyoto 606-8502, Japan

To understand how the direction of root growth changes in response to obstacles, light, and gravity, we characterized an *Arabidopsis thaliana* mutant, *wavy growth 2* (*wav2*), whose roots show a short-pitch pattern of wavy growth on inclined agar medium. The roots of the *wav2* mutant bent with larger curvature than those of the wild-type seedlings in wavy growth and in gravitropic and phototropic responses. The cell file rotations of the root epidermis of *wav2-1* in the wavy growth pattern were enhanced in both right-handed and left-handed rotations. *WAV2* encodes a protein belonging to the BUD EMERGENCE 46 family with a transmembrane domain at the N terminus and an α/β-hydrolase domain at the C terminus. Expression analyses showed that mRNA of *WAV2* was expressed strongly in adult plant roots and seedlings, especially in the root tip, the cell elongation zone, and the stele. Our results suggest that WAV2 is not involved in sensing environmental stimuli but that it negatively regulates stimulus-induced root bending through inhibition of root tip rotation.

INTRODUCTION

Roots of higher plants change their growth direction in response to various environmental stimuli, such as gravity, light, moisture, nutrients, temperature, and obstacles, to adapt to their environment and gain maximum advantage for growth. Since the pioneering studies of Darwin (1880), physiological and anatomical studies of root behavior triggered by several kinds of physical stimuli have been made. Recently, molecular genetic analysis of *Arabidopsis thaliana* has begun to shed light on the molecular mechanisms that regulate root growth, including gravitropism and phototropism (for review, see Okada and Shimura, 1994; Migliaccio and Piconese, 2001; Evans, 2003).

The response to obstacles that lie in the path of root growth was analyzed in Arabidopsis seedlings (Okada and Shimura, 1990). When Arabidopsis seedlings are grown on a hard-agar plate that is inclined 45° to the direction of gravity, the primary roots do not show straight growth as expected, but show a wavy growth pattern, as though the agar surface represented an obstruction to vertical growth. This wavy growth pattern is produced when the root tip grows alternately to the right and to the left of vertical. The root tip shows a periodic reverse of rotation, which is left-handed when the root is moving to the right (when looking at the plant from the shoot apex), and right-handed when the root is moving to the left.

To understand the mechanisms that induce root tip rotation and root bending in response to touching an obstruction, researchers have isolated several Arabidopsis mutants. The *wavy growth 1-1* (*wav1-1*) mutant produces mostly straight root growth with a few waves on an angled agar surface (Okada and Shimura, 1990); the mutant gene is allelic with *phototropin 1*/*root phototropism 1* (T. Sakai, unpublished results), which encodes a blue-light receptor that is required for root phototropism (Huala et al., 1997; Sakai et al., 2000). The gravitropic response of the primary root is reduced in the *long hypocotyl 5-1* mutant, in which the mutant gene encodes a transcriptional factor with a basic Leu zipper domain, and the roots also show straight growth on an inclined agar plate (Oyama et al., 1997). The *wav6-52* mutant shows a few waves; its mutant gene is allelic with the root gravitropism gene *agravitropic 1*/*pin-formed 2*, which encodes an auxin efflux carrier *AtPIN2* (Chen et al., 1998; Luschnig et al., 1998; Müller et al., 1998). The root gravitropism mutant *aux1* also shows straight growth (Okada and Shimura, 1990); its mutant gene encodes an auxin influx carrier (Bennett et al., 1996). Roots of mutant plants with a weak allele, *wav5-33*/*aux1-33*, sometimes form a circular path because the root tips rotate in one direction and are unable to reverse. Thus, normal phototropic and gravitropic responses may be necessary for pressing

[1] These authors contributed equally to this work.
[2] Current address: Department of Biology, Graduate School of Science, Kyushu University, 4-2-1 Ropponmatsu, Chuo-ku, Fukuoka 810-8560, Japan.
[3] Current address: RIKEN Plant Science Center, 1-7-22 Suehiro-cho, Tsurumi-ku, Yokohama, Kanagawa 230-0045, Japan.
[4] Current address: Department of Cellular Mechanisms and Functions, Graduate School of Bioagricultural Sciences, Nagoya University, Chikusa, Nagoya 464-8601, Japan.
[5] To whom correspondence should be addressed. E-mail tsakai@psc.riken.jp; fax 81-45-503-9591.
The author responsible for distribution of materials integral to the findings presented in this article in accordance with the policy described in the Instruction for Authors (www.plantcell.org) is: Tatsuya Sakai (tsakai@psc.riken.jp).
Article, publication date, and citation information can be found at www.plantcell.org/cgi/doi/10.1105/tpc.104.028530.

against an obstruction and for inducing the wavy growth pattern of the roots.

Mutants showing short-pitch waves in the roots were also isolated, but how this growth pattern is induced is mostly unknown. Mutants with a defect in Trp synthesis—*trp5-2*^{wvc1}, *trp3-1*, and *trp2-1*—show short-pitch waves (Rutherford et al., 1998). However, the function of this synthesis pathway in the wavy growth pattern is unknown. We previously reported the isolation of two mutants showing short-pitch waves, *wav2-1* and *wav3-1* (Okada and Shimura, 1990). In this report, we describe detailed characterization of the phenotypes of the *wav2* mutant, including the wavy growth pattern and the cell file rotation of roots, gravitropic and phototropic responses of roots, and microtubule organization and sensitivity to microtubule-affecting drugs. We also report the cloning and molecular characterization of the *WAV2* gene. We found that *WAV2*, which belongs to the *BUD EMERGENCE 46* (*BEM46*) gene family and encodes a transmembrane domain at the N terminus and an α/β-hydrolase domain at the C terminus, is involved in the suppression of the root bending in response not only to touch stimuli but also to gravity and light.

RESULTS

Characterization of the *wav2-1* Mutant

The *wav2-1* mutant displayed enhanced wavy root growth on inclined agar surfaces, as described previously (Figure 1A; Okada and Shimura, 1990). We measured the wave tangent angle (the angle between a tangent to the root growth direction and a hypothetical axis at each intersection between that axis and the root), wavelength, and growth rate of the wild-type roots (Landsberg *erecta* [L*er*]) and the *wav2-1* roots (Figures 1B to 1E). The roots of the *wav2-1* mutant had larger wave tangent angles and shorter wavelengths than the roots of the wild-type seedlings. The growth rates of the mutant roots were similar with that of the wild type. These results indicate that the mutation at the *WAV2* locus causes an abnormality in the root bending in response to the touch stimulus at the root tip but that it does not cause severe defects in the root growth.

Takahashi et al. (2002) reported that hydrotropic curvature was increased in the roots of *wav2-1*. We tested whether this mutant also shows abnormalities in response to gravity and light. When we examined the gravitropic response by inverting the agar medium, the wild-type roots showed gradual bending and a large radius of curvature, whereas the *wav2-1* roots showed sharp bending and a small radius (Figure 2A). When we changed the root direction from vertical to horizontal, the initial root curvature was larger in *wav2-1* than in the wild type in both horizontal positions (left and right) (Figure 2B). When we examined the phototropic response by unilateral irradiation with white light for 24 h, a slight but obvious enhancement of curvature was observed by irradiation from both the right and left in *wav2-1* (Figure 2C). Thus, angles of root curvature in *wav2-1* were larger than those in the wild type in positive gravitropism and negative phototropism, as well as in positive hydrotropism (Takahashi et al., 2002). Photosensors for phototropism are phototropin

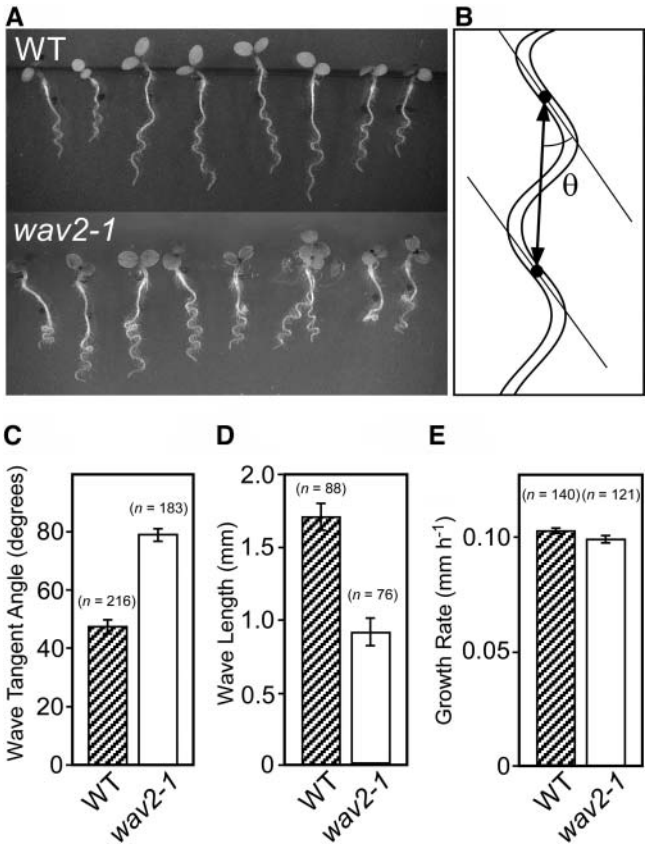

Figure 1. Comparison of Wild-Type and *wav2-1* Root Waving.

(A) Wild-type *A. thaliana* (L*er* ecotype) and *wav2-1* mutants that were grown for 2.5 d in the vertical position then for 3 d were tilted back at 45° on an agar surface.

(B) The wave tangent angle (θ) and wavelength (arrow) of a root.

(C) to **(E)** Quantification of root wave growth pattern of 5.5-d-old seedlings. Panels show the means ± SE of wave tangent angle **(C)**, wavelength **(D)**, and growth rate **(E)** of roots of the wild type and *wav2-1*. The growth rate of roots was calculated from the length of elongation of roots during the 72 h after the agar surface was inclined.

blue-light receptors (Briggs and Christie, 2002). Gravity sensors for gravitropism may sense the sedimentation of starch-filled amyloplasts (Blancaflor and Masson, 2003). The sensing mechanisms for light, gravity, touching, and moisture may all be different. Thus, these results suggest that WAV2 is a common regulator that suppresses root bending in response to various environmental stimuli but not a specific regulator that responds to touching or moisture.

A previous study suggested that the wavy growth pattern in roots is caused by periodic reversal of rotation of the root tip (Okada and Shimura, 1990). During wavy growth, right-turn root bending is accompanied by left-handed rotation of the root tip, and left-turn root bending is accompanied by right-handed rotation. Furthermore, the root tip rotation could be traced as the cell file rotation of the root epidermis (Okada and Shimura, 1990). To observe any effect of the *wav2-1* mutation on the root tip rotation, we quantified angles of cell file rotation (α) and root

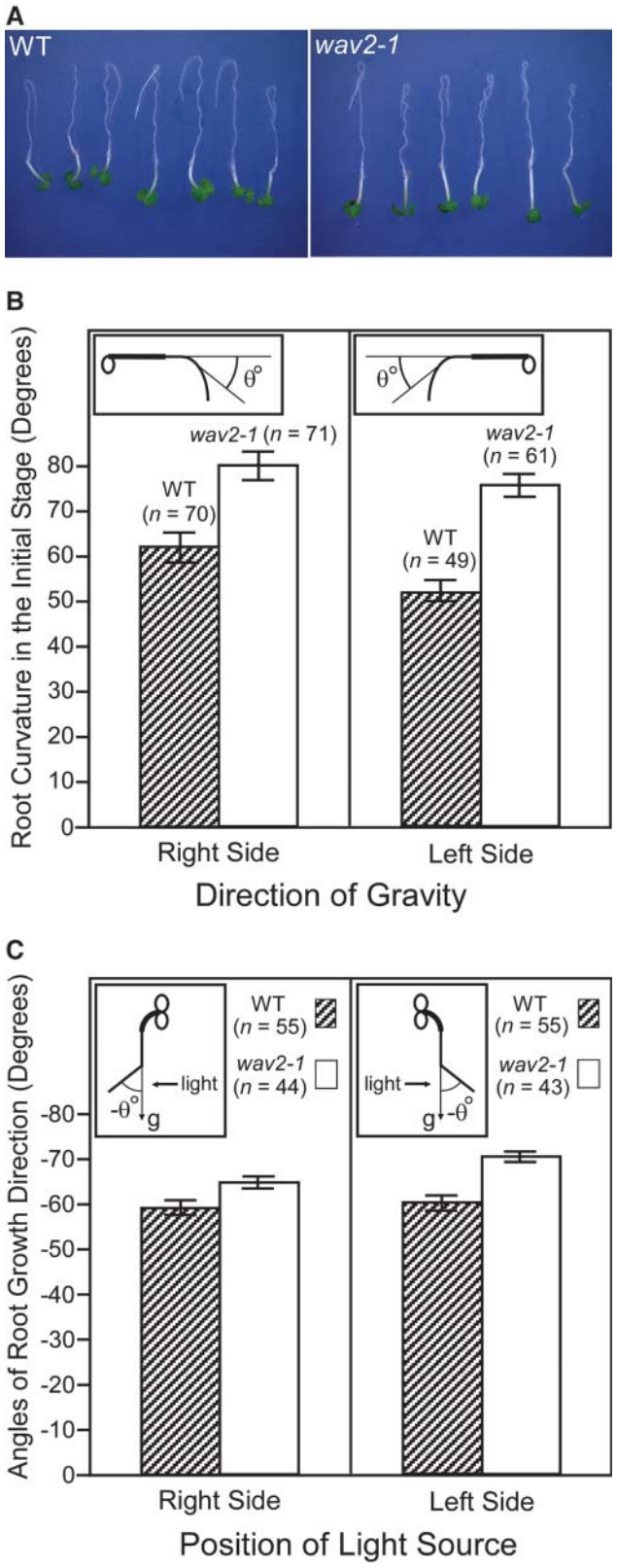

Figure 2. Root Gravitropism and Phototropism in Wild-Type (L*er*) and *wav2-1* Mutants.

(A) Root gravitropic response when the agar plate was shifted to the inverted position.

(B) Root gravitropic responses when the agar plate was shifted to the side positions. Initial curvatures of roots (θ°) were measured. Data and error bars represent the means of degrees ± SE.

(C) Root phototropic response. Angles of root growth direction against gravity (−θ°) were measured. Light was illuminated from either the right or the left side of the Petri dish. Data and error bars represent the means of degrees ± SE.

bending (β) in 100-μm segments of root within the first three and a half waves (Figure 3; see Methods). Both variables were greater in *wav2-1* (Figures 3E and 3F) than in the wild type (Figures 3C and 3D). As Okada and Shimura (1990) described previously, the right-handed cell file rotation (–α) occurred before the left-turn root bending (–β), and the left-handed cell file rotation (+α) occurred before the right-turn root bending (+β) in all waves of root growth (Figures 3C to 3F), except in the first bend of a *wav2-1* seedling (Figure 3F). These results suggest that the enhancement of cell file rotation causes the increase of root bending in the *wav2-1* mutant.

Cortical Microtubules and Effects of Microtubule-Affecting Drugs

Recent studies indicate that the organization of cortical microtubules is involved in the regulation of root tip rotation (Hashimoto, 2002; Lloyd and Chan, 2002). To determine how cortical microtubules array in root epidermal cells of wild-type and *wav2* seedlings showing wavy growth pattern, whole-mount immunostaining experiments were performed on those seedlings. In both of *wav2-1* and wild-type roots, the cortical microtubule arrays appeared to be mostly transverse throughout the entire main and distal elongation zones; there were no noticeable differences between roots of wild-type and *wav2-1* (Figure 4).

Next, we examined the sensitivity of roots to drugs that affect microtubules by measuring the root slanting angles on agar medium in the vertical position (Figure 5A). When 0.5 to 5 μM propyzamide, a microtubule-destabilizing chemical, was added to the growth medium, wild-type roots showed an exaggerated rightward slant (Figure 5B, positive angles) through left-handed cell file rotation (data not shown), as described previously (Furutani et al., 2000). The *wav2-1* roots also slanted rightward, but less than the wild type in both the absence and the presence of propyzamide, indicating a slight resistance to the drug (Figure 5B). When 0.1 and 0.3 μM taxol, a microtubule-stabilizing chemical, was added to the growth medium, wild-type roots showed a reduced rightward slant (Figure 5C). *wav2-1* showed a higher sensitivity to taxol, and 0.3 μM taxol caused a slightly leftward root slant (Figure 5C), in which the root tip of the mutant seedlings sometimes showed right-handed rotation (data not shown). A reversal of the trend in root slanting was observed by taxol at 1 μM, as compared with 0.1 and 0.3 μM, in both seedlings, and root slanting angle of *wav2-1* was smaller than that of the wild type at 1 μM, as well as at 0.1 or 0.3 μM (Figure 5C). Although 3 μM taxol inhibited germination and caused growth defects in

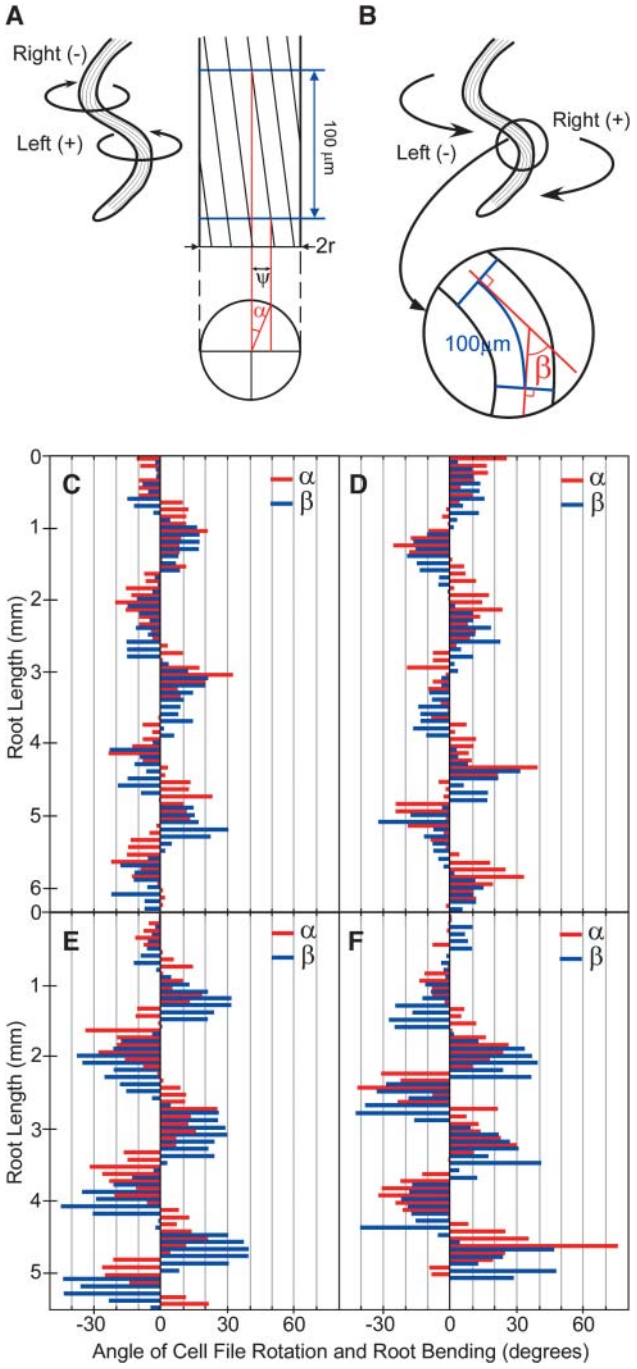

Figure 3. Quantification of Cell File Rotation and Root Bending.

(A) and **(B)** Illustrations show angles of cell file rotation (α) and root bending (β) within a 100-μm segment of the waving root. See Methods for details. Positive values represent left-handed cell file rotation and right-turn root bending; negative values represent right-handed cell file rotation and left-turn root bending.

(C) to **(F)** Angles of cell file rotation (α) and root bending (β) in two wild-type (**[C]** and **[D]**) and two *wav2-1* seedlings (**[E]** and **[F]**). Root length is the distance from the starting point of root bending. Six seedlings of each line were measured; panels show two typical seedlings of each.

many seedlings, surviving seedlings showed a strong rightward slant in wild-type and *wav2-1* (33.3 ± 2.0° in the wild type [means ±SE; $n = 21$] and 25.1 ± 1.6° in *wav2-1* [means ±SE; $n = 24$]). Reduction of rightward slant by 0.1 and 0.3 μM taxol and enhancement of rightward slant by taxol at 1 μM or more were also seen by Furutani et al. (2000) with wild-type seedlings.

Figure 4. Confocal Micrographs of Cortical Microtubules in Root Epidermal Cells of the Wild Type and *wav2-1* Mutant.

(A) and **(B)** Montages of image of cortical microtubules in a root of the wild type **(A)** and *wav2-1* **(B)**.

(C) and **(D)** Closer views within a root main elongation zone of the wild type **(C)** and *wav2-1* **(D)**.

(E) and **(F)** Closer views within a root distal elongation zone of the wild type **(E)** and *wav2-1* **(F)**.

Bars = 20 μm (**[A]** and **[B]**) and 10 μm (**[C]** to **[F]**).

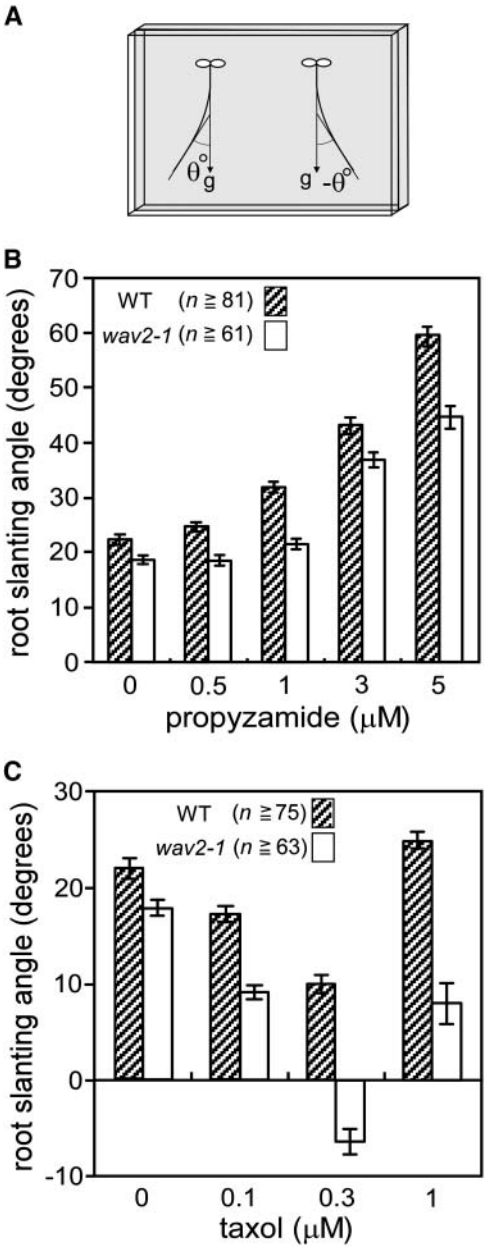

Figure 5. Effects of Propyzamide and Taxol on the Root Growth Direction in the Wild Type (L*er*) and *wav2-1* Mutant.

(A) Root slanting angles (θ) against gravity (g). Rightward- and leftward-slanting angles are represented as positive and negative values, respectively.
(B) and **(C)** Root slanting angles of 5-d-old seedlings of the wild type and *wav2-1* on agar medium containing propyzamide **(B)** or taxol **(C)**. Data and error bars represent means ± SE.

Cloning of *WAV2*

To understand the molecular nature of the *WAV2* gene product, we determined the gene structure using a map-based cloning procedure. *WAV2* was mapped to a 123-kb region of chromosome 5, with a region that includes putative genes from Arabidopsis Genome Initiative loci At5g20240 to At5g20560 (Figure 6A). All annotated genes in this region of the *wav2-1* mutant were sequenced; only one base change was found, in At5g20520. A full-length cDNA corresponding to the open reading frame of At5g20520 was obtained from the Arabidopsis Biological Resource Center's cDNA catalog. The 5′-noncoding region of this gene was confirmed by the rapid amplification of cDNA 5′-ends method (data not shown). Normal wavy growth of roots was recovered in a transgenic *wav2-1* mutant, named *wav2-1-Hin*cII,

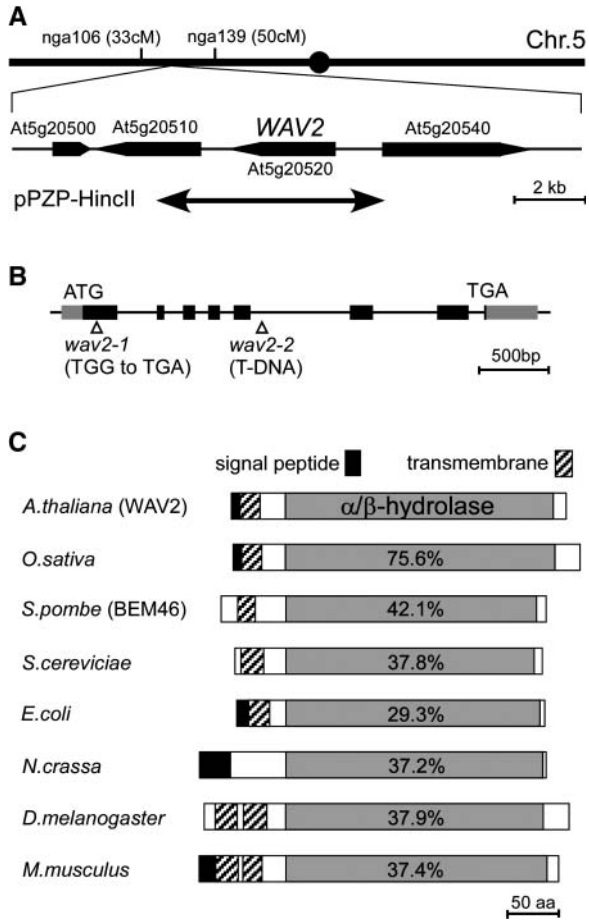

Figure 6. Identification of the *WAV2* Gene and Structure of Proteins of the BEM46/WAV2 Family.

(A) Map-based cloning of *WAV2*. The mutated locus in *wav2-1* was mapped between markers nga106 and nga139 on chromosome 5. Black boxes indicate the *WAV2* genes and predicted genes around it. The arrow shows a region covered by a restriction DNA fragment isolated from BAC clone F7C8, which is cloned in the pPZP211 binary vector for use in the complementation assay. cM, centimorgan.
(B) Genome structure of *WAV2*. Black rectangles, protein-coding regions; white rectangles, noncoding regions. Triangles indicate the point mutation site in *wav2-1* and the insertion site of T-DNA in *wav2-2*.
(C) Structure of the BEM46/WAV2 family. Percentages show amino acid similarity in the α/β-hydrolase domain between the deduced amino acid sequence of each gene and that of *WAV2*. aa, amino acids.

Table 1. Wavy Root Growth Pattern in Wild-Type Seedlings (L*er* and Ws), *wav2-1* and *wav2-2* Mutants, and a Transgenic *wav2-1* Mutant with Restored Function (*wav2-1-Hin*cII)

Strain	Wave Tangent Angles (°; mean ± SE)	Wavelength (mm; mean ± SE)	Growth Rate (mm h^{-1}; mean ± SE)
L*er*	48.4 ± 1.0 ($n = 216$)	1.7 ± 0.1 ($n = 88$)	0.103 ± 0.002 ($n = 140$)
wav2-1	79.4 ± 1.3 ($n = 183$)	0.9 ± 0.1 ($n = 76$)	0.100 ± 0.002 ($n = 121$)
*wav2-1-Hin*cII	47.4 ± 1.4 ($n = 181$)	1.86 ± 0.08 ($n = 76$)	0.098 ± 0.003 ($n = 67$)
Ws	33.3 ± 1.9 ($n = 91$)	1.55 ± 0.04 ($n = 70$)	0.122 ± 0.003 ($n = 87$)
wav2-2	57.0 ± 1.7 ($n = 102$)	1.15 ± 0.04 ($n = 68$)	0.127 ± 0.006 ($n = 95$)

which carried a genomic DNA fragment containing At5g20520 (Table 1). The *wav2-2* mutant, carrying a T-DNA insertion in At5g20520 of the Wassilewskija (Ws) ecotype, showed a shorter wave pitch than that of the Ws wild-type seedlings, although the pitch was weaker than that of the *wav2-1* mutant (Table 1). We concluded that the gene is *WAV2*.

WAV2 contains eight exons and encodes a predicted protein of 308 amino acid residues with a molecular mass of 34 kD (Figure 6B). The *wav2-1* gene possesses a non-sense mutation at residue 70 (TGG [Trp] to TGA [stop]), suggesting that the *wav2-1* mutation is null. The WAV2 protein possesses a signal peptide with a transmembrane domain at its N terminus and an α/β-hydrolase domain in the middle of the protein (Figure 6C). BLAST searches revealed that *WAV2* belongs to the *BEM46* gene family in the α/β-hydrolase superfamily (Figure 6C). It is a unique gene in the Arabidopsis genome, but homologous genes were identified in *Oryza sativa*, *Schizosaccharomyces pombe* (*BEM46*), *Saccharomyces cerevisiae* (YNL320W), *Escherichia coli*, *Neurospora crassa*, *Drosophila melanogaster*, and *Mus musculus*. The *BEM46* gene of *S. pombe* is registered as a suppressor of the *bem1/bud5* mutants of *S. cerevisiae* in the *S. pombe* Gene Database (http://www.genedb.org/genedb/pombe/), but its molecular function has not been identified yet.

Expression Patterns of the *WAV2* Gene

The expression pattern of the transcripts of *WAV2* was revealed by RNA gel blot analysis. Stronger expression was detected in young seedlings and in roots of adult plants than in stems, leaves, and flowers (Figure 7).

The expression pattern in roots was observed using a green fluorescent protein (GFP) reporter gene. When the GFP-fused WAV2 protein (WAV2:GFP) was induced by the *WAV2* gene promoter, it complemented the *wav2-1* mutation and thus functioned normally (data not shown). The root tip, including the cell elongation zone and the stele, showed the brightest GFP fluorescence in this transgenic *wav2-1* mutant (Figures 8A to 8D), although fluorescence was observed in all root tissues (Figure 8A), and slight fluorescence was detected in the hypocotyls and cotyledon (data not shown). The expression in the root tip seemed to be consistent with the function of WAV2 in regulating root tip rotation.

Because WAV2 has a putative transmembrane domain in its N-terminal region, it seems to be a membrane protein. When the subcellular localization of WAV2:GFP proteins was observed, fluorescence was detected at the surface of cells and inside of cells except in the nucleus or vacuoles (Figure 8E). Gaps in fluorescence were observed in the apoplast (Figure 8F), suggesting that the WAV2:GFP protein does not diffuse into the apoplast. To determine whether WAV2:GFP was localized to the cell wall, we treated roots with 1 M mannitol to plasmolyze the cells. Confocal images of these roots showed a considerable amount of fluorescence within the cell as WAV2:GFP pulled away from the cell wall during plasmolysis (Figures 8G and 8H), indicating that fluorescence was not localized to the cell wall and that WAV2 was not secreted from cell to apoplast. To know whether the WAV2:GFP proteins are localized in cytoplasm or membranes, we prepared the soluble fraction and the crude microsomal fraction from whole seedlings and roots of seedlings expressing WAV2:GFP and analyzed both fractions by a immunoblot with an anti-GFP antibody. WAV2:GFP was detected, as an ~60-kD band, in the crude microsomal fraction but not in the soluble fraction prepared from both whole seedlings and roots (Figure 9). Preparations of the soluble fraction were confirmed by anti-glutamine synthetase (GS) 1 antibody (Figure 9), which reacts with the 40-kD polypeptide of cytosolic GS protein in Arabidopsis (H. Sakakibara, personal communication). From the results of observation of GFP fluorescence and immunoblot analysis, we concluded that the WAV2 proteins localize in the plasma membrane and membranes of inner membrane compartments but not in cytoplasm, nucleus, vacuoles, and apoplast.

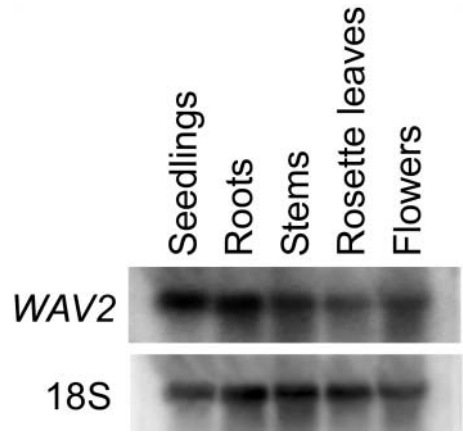

Figure 7. RNA Gel Blot Analysis of *WAV2* Gene Expression.

Probes were specific for *WAV2* and 18S rRNA as a loading control.

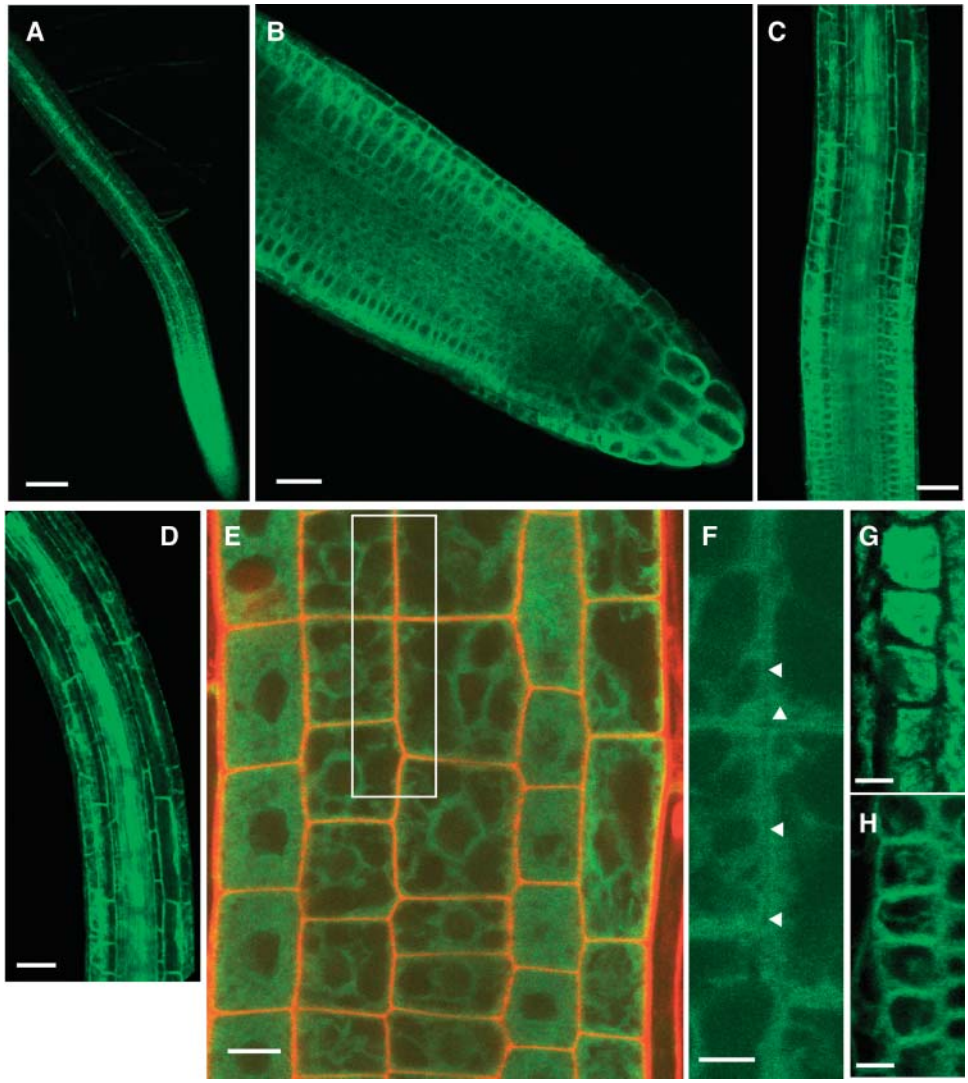

Figure 8. Confocal Images of Fluorescence in Transgenic *wav2-1* Seedlings Expressing a WAV2:GFP Fusion Protein.

(A) to **(D)** Roots of transgenic *wav2-1* seedlings expressing WAV2:GFP. Images show root **(A)**, root tip **(B)**, elongation zone **(C)**, and upper region of elongation zone **(D)**.
(E) A composite image of WAV2:GFP (green fluorescence) with cell walls stained with propidium iodide (red fluorescence) in elongation zone.
(F) High-magnification image of WAV2:GFP indicated as a white square in **(E)**. Arrowheads indicate gaps in fluorescence at the apoplasts.
(G) Plasmolyzed cells of the root tip of the transgenic *wav2-1* seedlings expressing the WAV2:GFP protein.
(H) Control image of the WAV2:GFP protein before the plasmolyzation.
Bars = 100 μm **(A)**, 20 μm **(B)**, 40 μm (**[C]** and **[D]**), 10 μm **(E)**, 5 μm **(F)**, and 10 μm (**[G]** and **[H]**).

DISCUSSION

Function of WAV2 in Root Bending and Root Tip Rotation

In this study, we have characterized phenotypes of the *wav2* mutant in detail. Roots of the *wav2* mutant bend at a greater angle during wavy growth and in gravitropic and phototropic bending (Figures 1 and 2), as well as in hydrotropic bending (Takahashi et al., 2002). These results strongly suggest that the WAV2 protein is not involved in sensing environmental stimuli (touch, moisture, gravity, and light) but that it negatively regulates root bending when roots alter their growth direction.

The cell file rotations of *wav2-1* roots in the wavy growth pattern were enhanced in both right- and left-handed rotations (Figure 3). Our observations suggest that the enhancement of root bending in the wavy growth pattern of *wav2-1* is caused by the enhancement of cell file rotation. We also tried to observe the enhancement of cell file rotation in the gravitropic and phototropic curvatures of *wav2* roots; the pattern of cell file rotation is intricate, and we could not reach conclusions about the

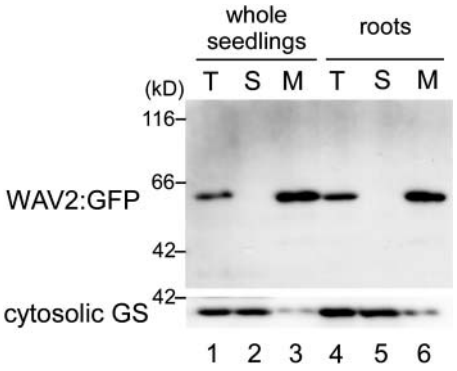

Figure 9. Immunoblot of WAV2:GFP Fusion Protein.

Fractions of total proteins (T; lanes 1 and 4), soluble proteins (S; lanes 2 and 5), and crude microsomal proteins (M; lanes 3 and 6) were prepared from whole seedlings (lanes 1 to 3) and roots of seedlings (lanes 4 to 6) expressing WAV2:GFP. Proteins (10 μg for lanes 1 to 3 and 5 μg for lanes 4 to 6) in each fraction were separated on a 10% SDS-polyacrylamide gel followed by immunoblotting with anti-GFP antibody. Anti-glutamine synthetase (GS) 1 antiserum, which recognizes GS localized in cytoplasm, was used as a marker for cytosolic proteins.

relationship between the enhancement of root bending in gravitropic and phototropic responses and the enhancement of cell file rotation (data not shown). Buer et al. (2003) and Sedbrook et al. (2004) reported that wild-type Arabidopsis roots sometimes show the wavy growth pattern without the root tip rotation and that differential growth between cells in a concave side and in a convex side of root bending also may be involved in wavy growth. It is possible that WAV2 plays a role in regulation of differential growth of roots, in addition to the regulation of root tip rotation during root bending.

Microtubule Organization and WAV2

Recent studies suggested that the orientation of cortical microtubule arrays in epidermal cells is important for root tip rotation (Hashimoto, 2002). *spiral 1* (*spr1*) and *spr2* mutants show constitutive right-handed cell file rotation in roots (Furutani et al., 2000), and *lefty 1* and *lefty 2* mutants show constitutive left-handed cell file rotation in roots (Thitamadee et al., 2002). Cortical microtubules in elongating epidermal cells of *spr1-1* roots were arranged in left-handed helical arrays, and those of *lefty* roots were arranged in right-handed obliquely oriented arrays. From those results, Hashimoto (2002) proposed that cortical microtubule arrays determine the handedness of rotating organs. To examine the involvement of WAV2 in microtubule organization, we examined the orientation of cortical microtubule arrays and sensitivity to microtubule-affecting drugs in the *wav2-1* mutant. The orientation of cortical microtubule arrays in the *wav2-1* mutants looked normal in the root elongation zone (Figure 4). We did not detect radial swelling, which is caused by an abnormality of microtubule organization (Whittington et al., 2001; Hashimoto, 2002), in *wav2-1* roots during wavy growth, and this mutant did not show an abnormal root growth rate (Figure 1E). The WAV2 protein does not possess any known microtubule binding motif, and its subcellular localization did not show any correlation with microtubule arrays (Figures 5 and 8E). Although the *wav2-1* seedlings showed resistance to propyzamide in rightward root slanting (Figure 5B) and greater suppression of the rightward root slanting by low concentrations of the microtubule-stabilizing taxol than that of wild-type seedlings (Figure 5C), these results are not enough to indicate the involvement of WAV2 in the stability and/or dynamics of microtubules. Because the rightward slanting in *wav2-1* was weaker than that of the wild type in the absence of propyzamide (Figure 5B), it is possible that these differences are generated by a defect in some mechanism other than the microtubule organization. On the other hand, SPR2/TOR1 is a microtubule-associated protein and seems to regulate microtubular organization (Buschmann et al., 2004), although the microtubule arrays of the *spr2/tor1* mutant are mostly indistinguishable from those of the wild type, and the mutant showed no phenotype in studies of microtubule-affecting drugs (Furutani et al., 2000). A *spr1* allele, *spr1-6/sku6-1*, also shows normal orientation of microtubule arrays (Sedbrook et al., 2004). Thus, we cannot reach conclusions about the function of WAV2 in the microtubule organization just by observation of microtubule arrays, so the question remains.

Function of the BEM46/WAV2 Family

We have revealed that *WAV2* encodes a protein belonging to the BEM46 family within the α/β-hydrolase superfamily. The α/β-hydrolase domain is common to several hydrolytic enzymes of widely differing phylogenetic origins and catalytic functions (Nardini and Dijkstra, 1999). It is yet unknown whether the proteins encoded by this family have hydrolase activity and on what kind of substrate they operate. The *S. pombe BEM46* gene was originally registered as a suppressor of *S. cerevisiae bem1* and *bud5* mutants. *bem1* and *bud5* show a defect in a cell polarization and establishment of nonrandom budding patterns (Cabib et al., 1998; Madden and Snyder, 1998). BUD5 is a GTP–GDP exchange factor (GEF) for BUD1 Ras-like small G protein and is necessary for bud site selection (Chant et al., 1991). BEM1 is a scaffold protein binding to BUD1, to the Cdc24p GEF for the Cdc42p Rho-like small G protein, to GTP-CDC42p, and to actin (Park et al., 1997; Cabib et al., 1998; Irazoqui et al., 2003). The *BEM46*-homologous gene YNL320W is a single-copy gene in *S. cerevisiae* but is not essential (Giaever et al., 2002), similar to *WAV2* in Arabidopsis. Global analysis of protein interactions in *D. melanogaster* indicated that there is a low-confidence interaction between Drosophila BEM46 and RAPSYNOID (Giot et al., 2003), which is a putative GEF for Gα protein and is involved in the control of asymmetric cell divisions (Parmentier et al., 2000). One working hypothesis on the molecular function of the BEM46 family is that the members modulate the function of some morphogenic determinants, like GEF or actin, on the cell surface.

Expression Patterns and Subcellular Localization of WAV2

The expression of *WAV2* mRNA in roots of adult plants growing on soil suggested that WAV2 also regulates the growth pattern change of adult roots in soil, as well as of seedling roots on agar

medium. mRNA of *WAV2* was also expressed in the stem. In addition, when fluorescence signals were visible in the seedlings expressing WAV2:GFP (driven by the *WAV2* gene promoter), slight expression was also detected in hypocotyls. Although we did not find any remarkable defect in the growth of hypocotyls and inflorescence stems of the *wav2* mutants, WAV2 might regulate the growth of hypocotyls and stems in response to environmental stimuli, similar to that of roots.

Our analysis using GFP fusion protein suggests that WAV2 does not localize in the apoplast, cytoplasm, nucleus, or vacuoles of cells but that it localizes in the plasma membrane and membranes of some organelles (Figures 8 and 9). The WAV2 protein has a signal peptide and one transmembrane domain in its N terminus, and its subcellular localization is consistent with a result predicted from its protein structure. Although the involvement of WAV2 in root tip rotation and the sensitivity to the microtubule-affecting drugs suggest an interaction of WAV2 with microtubules, the GFP fluorescence was not related to the cortical microtubule array, but instead was observed all over the surface of the cell. Identification of WAV2-associated proteins at the membranes will help to elucidate the function of WAV2 to regulate the cell morphogenesis in response to various environmental stimuli, including touching, gravity, light, and moisture.

METHODS

Plant Growth Conditions and Microscopy

Arabidopsis thaliana seeds were sterilized with 10% (v/v) bleach with 0.02% (v/v) Triton X-100 for 5 min. After five washes in sterilized water, seeds were germinated and grown on square Petri dishes containing half-strength Okada and Shimura medium (Okada and Shimura, 1990) with 1.5% (w/v) agar. After sowing, dishes were wrapped with Micropore surgical tape (3M Health Care, St. Paul, MN). The dishes were then kept in darkness at 4°C for 2 to 4 d. Then they were transferred to a growth chamber at 22°C under constant white light (a white fluorescent lamp model FL20S-EXNH; Toshiba, Tokyo, Japan). For observation of the wavy growth pattern of roots, Petri dishes were positioned vertically for the first 2.5 d of seedling growth and then inclined backward 45° for 3 to 5 d. For observation of the gravitropic response of roots in the inverted position, dishes were positioned vertically for the first 4 d and were inverted for the next 3 d. For observation of the gravitropic response of roots in the side positions, dishes were positioned vertically for the first 2 d and were changed to the side position for the next 2 d in the dark. For measurement of the phototropic response of roots, seedlings on the surface of agar medium in the vertical position were exposed to white light for 60 h and then irradiated from one side by white light at 100 μmol m^{-2} s^{-1} for 24 h. Seedling images were obtained with a three-dimensional digital fine scope (VC4500-PC; Omron, Tokyo, Japan) or digital microscope (VH-8000; Keyence, Osaka, Japan).

Quantification of Cell File Rotation and Root Bending

For quantification of angles of cell file rotation (α) and of root bending (β), roots of 5.5-d-old seedlings showing the wavy growth pattern were photographed at high magnification ($\times$100). The starting point of the first wave was determined from observations of root bending. The values of α and β were measured on each 100-μm segment in the first 3.5 waves. The value of α was calculated from the gap of position of a cell file between top and bottom of a 100-μm segment, assuming that the root is a cylinder, as α (°) = 90 – arccos(ψ/*r*), where ψ is the distance of the position from the center line of the root, *r* is the radius of the root, and β is the angular difference of root growth direction in each 100-μm segment (Figures 3A and 3B).

Whole-Mount Immunostaining of Cortical Microtubules

Seedlings showing wavy root growth were examined. Microtubules of seedling roots were immunostained as described (Sugimoto et al., 2000), with some modification. Cellulase (0.1%) Onozuka RS (Yakult Honsha, Tokyo, Japan) was added to the 0.05% pectolyase Y-23 (Kikkoman, Tokyo, Japan) enzyme solution, 1% BSA, 50 mM Gly in PBS was treated for 30 min before a treatment of primary antibody, and root tissues were mounted in an agent of Slowfade light antifade kit (Molecular Probes, Eugene, OR). We used monoclonal anti-α-tubulin antibody (clone DM1A; Sigma-Aldrich, St. Louis, MO) diluted 1:800 with 50 mM Gly in PBS buffer (50 mM $NaPO_4$, pH 7.0), as a primary antibody, and fluorescein-labeled antibody to mouse IgG (Kirkegaard and Perry Laboratory, Gaithersburg, MD) diluted 1:100 with 50 mM Gly in PBS buffer as a secondary antibody. Fluorescence was visualized using a confocal laser-scanning microscope (LSM510 META version 3.2; Zeiss, Fotografieren, Germany) attached to a microscope (Axioplan2; Zeiss). Several seedlings were observed, and results were confirmed.

Map-Based Cloning of *WAV2*

We crossed *wav2-1* (L*er* ecotype; Okada and Shimura, 1990) with Columbia (Col) wild type and selected F2 seedlings by screening for short-pitched wavy root growth on agar plates inclined at 45° to the vertical. Genomic DNA from individual F2 seedlings was isolated and amplified with primers for various PCR-based cleaved amplified polymorphisms and simple sequence length polymorphism markers, including nga106 and nga139, and designed by single nucleotide polymorphism in the Cereon Arabidopsis Polymorphism Collection (Jander et al., 2002), then assayed for L*er*- and Col-specific polymorphisms. ExTaq polymerase (TaKaRa Bio, Ohtsu, Japan) was used for PCR. Nucleotide sequences were determined using an ABI3100 genetic analyzer and Big Dye Terminator sequencing kit version 3 (Applied Biosystems, Foster City, CA). Sequence data were analyzed by GENETYX-MAC 11.2.5 (Software Development, Tokyo, Japan).

For complementation analysis, we cloned a *Hinc*II-digested 6.2-kb fragment of the F7C8 BAC including the *WAV2* gene into the binary vector pPZP211 (Hajdukiewicz et al., 1994). This plasmid, pPZP-*Hinc*II, was used for transformation of *Agrobacterium tumefaciens* ASE strain, which was used for a floral dip of *wav2-1* plants (Clough and Bent, 1998). Transgenic plants were selected on MS medium (Wako Chemicals, Osaka, Japan) containing 50 μg/mL of kanamycin. The wavy phenotypes of roots of T3 plants were examined. Several transgenic lines carrying pPZP-*Hinc*II showed complementation of the *wav2* mutation. We used the SMART computer program (http://coot.embl-heidelberg.de/SMART) to analyze the structure of the WAV2 protein.

The F7C8 BAC clone and the *WAV2* cDNA clone 171E17 were obtained from the Arabidopsis Biological Resource Center. The *wav2-2* mutant (Ws ecotype) was screened from seeds of T-DNA insertion line pool number CSJ1123 from the Arabidopsis Functional Genomics Consortium.

RNA Gel Blot Analysis

Total RNA was isolated from roots, stems, rosette leaves, and flowers of adult plants and from 5-d-old-seedlings of L*er* using the RNeasy plant mini kit (Qiagen, Tokyo, Japan) or Isogen (Nippongene, Tokyo, Japan). Total RNA (30 μg) was loaded onto each lane of denaturing agarose gel, electrophoresed, transferred to a nylon membrane (Biodyne B membrane; Pall, Port Washington, NY), and hybridized with radioactive

random-primed DNA prepared with *WAV2* cDNA as a template. To confirm the amount of RNA in each lane, we also hybridized a DNA probe complementary to 18S rRNA with the membrane. BAS MS-2040 imaging plates and cassettes (Fuji Photo Film, Tokyo, Japan) were used for detection of hybridization. The hybridization signals were visualized with a Typhoon variable image analyzer (Amersham Biosciences, Buckinghamshire, UK).

GFP Imaging

The *WAV2* promoter:*WAV2*:GFP gene was constructed within binary vector pPZP211. Approximately 2.8 kb of a restriction DNA fragment from the *Hinc*II site in the *WAV2* gene promoter region to the *Xba*I site in the 5th exon was obtained from pPZP-*Hinc*II, which was used for the complementation analysis. Part of the *WAV2* cDNA from the 5th to the 7th exon was amplified by PCR and checked by DNA sequencing. The *WAV2* genome DNA and a part of its cDNA were fused with the GFP gene. This construct encoded all amino acid residues of WAV2 except the last one. The construct was introduced into the *wav2-1* mutant by *A. tumefaciens*–mediated transformation. T2 and T3 seedlings with the complemented wavy growth phenotype were floated on 1 μg/mL of propidium iodide for 4 min to stain the cell walls. GFP fluorescence was visualized in whole mounts using a confocal laser-scanning microscope (LSM5 Pascal version 3.2; Zeiss) with the fluorescein isothiocyanate channel (green, GFP) and the rhodamine channel (red, propidium iodide). Cells were plasmolyzed by treating seedlings with 1 M mannitol for 60 s.

Protein Extraction and Immunoblot Analysis

Seven-day-old seedlings showing the wavy growth pattern of roots were harvested from inclined agar medium with forceps. Roots of 7-d-old seedlings were also harvested. Total protein extracts, soluble fraction, and crude microsomal fraction were prepared as described by Inada et al. (2004). Anti-GFP antibody (mouse monoclonal antibody, clone GF200) was obtained from Nacalai Tesque (Kyoto, Japan). Anti-glutamine synthetase (GS) 1 antiserum was described by Sakakibara et al. (1992). Horseradish peroxidase (HRP)–conjugated anti-mouse IgG antibody and HRP-conjugated anti-rabbit IgG antibody were obtained from Amersham Biosciences (Piscataway, NJ). HRP activity was detected by the ECL advance protein gel blotting detection kit (Amersham Biosciences) and imaged on the x-ray film (Hyperfilm ECL; Amersham Biosciences). Immunoblot analysis was done twice on independent samples, and the result was confirmed.

Sequence data of the BEM46 family have been deposited with the DDBJ/EMBL/GenBank data libraries under accession numbers AB182157 (*A. thaliana*; *WAV2*), AK106096 (*O. sativa*), U29892 (*S. pombe*; *BEM46*), Z71596 (*S. cerevisiae*; YNL320W), AF069781 (*D. melanogaster*; AF069781), and BC043690 (*M. musculus*) and with the TrEMBL data library under accession numbers for hypothetical amino acid sequences of the family, P77538 (*E. coli*) and Q7SDX9 (*N. crassa*).

ACKNOWLEDGMENTS

We thank Hitoshi Sakakibara for providing anti-GS1 antiserum, Yasuo Niwa for providing the GFP gene, Ikuyo Furutani for critical advice on visualization of cortical microtubules, the Arabidopsis Biological Resource Center for providing the F7C8 BAC clone and the 171E17 clone, and the Arabidopsis Functional Genomics Consortium for screening and providing the *wav2-2* mutant.

Received October 11, 2004; accepted November 25, 2004.

REFERENCES

Bennett, M.J., Marchant, A., Green, H.G., May, S.T., Ward, S.P., Millner, P.A., Walker, A.R., Schultz, B., and Feldmann, K.A. (1996). *Arabidopsis AUX1* gene: A permease-like regulator of root gravitropism. Science **273,** 948–950.

Blancaflor, E.B., and Masson, P.H. (2003). Plant gravitropism. Unraveling the ups and downs of a complex process. Plant Physiol. **133,** 1677–1690.

Briggs, W.R., and Christie, J.M. (2002). Phototropin 1 and 2: Versatile plant blue-light receptors. Trends Plant Sci. **7,** 204–210.

Buer, C.S., Wasteneys, G.O., and Masle, J. (2003). Ethylene modulates root-wave responses in Arabidopsis. Plant Physiol. **132,** 1085–1096.

Buschmann, H., Fabri, C.O., Hauptmann, M., Hutzler, P., Laux, T., Lloyd, C.W., and Schäffner, A.R. (2004). Helical growth of the *Arabidopsis* mutant *tortifolia1* reveals a plant-specific microtubule-associated protein. Curr. Biol. **14,** 1515–1521.

Cabib, E., Drgonová, J., and Drgon, T. (1998). Role of small G proteins in yeast cell polarization and wall biosynthesis. Annu. Rev. Biochem. **67,** 307–333.

Chant, J., Corrado, K., Pringle, J.R., and Herskowitz, I. (1991). Yeast *BUD5*, encoding a putative GDP-GTP exchange factor, is necessary for bud site selection and interacts with bud formation gene *BEM1*. Cell **65,** 1213–1224.

Chen, R., Hilson, P., Sedbrook, J., Rosen, E., Caspar, T., and Masson, P.H. (1998). The *Arabidopsis thaliana AGRAVITROPIC1* gene encodes a component of the polar-auxin-transport efflux carrier. Proc. Natl. Acad. Sci. USA **95,** 15112–15117.

Clough, S., and Bent, A.F. (1998). Floral dip: A simplified method for *Agrobacterium*-mediated transformation of *Arabidopsis thaliana*. Plant J. **16,** 735–743.

Darwin, C. (1880). The Power of Movement in Plants. (London: John Murray).

Evans, M. (2003). Touch sensitivity in plants: Be aware or beware. Trends Plant Sci. **8,** 312–314.

Furutani, I., Watanabe, Y., Prieto, R., Masukawa, M., Suzuki, K., Naoi, K., Thitamadee, S., Shikanai, T., and Hashimoto, T. (2000). The *SPIRAL* genes are required for directional control of cell elongation in *Arabidopsis thaliana*. Development **127,** 4443–4453.

Giaever, G., et al. (2002). Functional profiling of the *Saccharomyces cerevisiae* genome. Nature **418,** 387–391.

Giot, L., et al. (2003). A protein interaction map of *Drosophila melanogaster*. Science **302,** 1727–1736.

Hajdukiewicz, P., Svab, Z., and Maliga, P. (1994). The small, versatile pPZP family of *Agrobacterium* binary vectors for plant transformation. Plant Mol. Biol. **25,** 989–994.

Hashimoto, T. (2002). Molecular genetic analysis of left–right handedness in plants. Philos. Trans. R. Soc. Lond. B Biol. Sci. **357,** 799–808.

Huala, E., Oeller, P.W., Liscum, E., Han, I.S., Larsen, E., and Briggs, W.R. (1997). *Arabidopsis* NPH1: A protein kinase with a putative redox-sensing domain. Science **278,** 2120–2123.

Inada, S., Ohgishi, M., Mayama, T., Okada, K., and Sakai, T. (2004). RPT2 is a signal transducer involved in phototropic response and stomatal opening by association with phot1. Plant Cell **16,** 887–896.

Irazoqui, J.E., Gladfelter, A.S., and Lew, D.J. (2003). Scaffold-mediated symmetry breaking by Cdc42p. Nat. Cell Biol. **5,** 1062–1070.

Jander, G., Norris, S.R., Rounsley, S.D., Bush, D.F., Levin, I.M., and Last, R.L. (2002). Arabidopsis map-based cloning in the post-genome era. Plant Physiol. **129,** 440–450.

Lloyd, C., and Chan, J. (2002). Helical microtubule arrays and spiral growth. Plant Cell **14,** 2319–2324.

Luschnig, C., Gaxiola, R.A., Grisafi, P., and Fink, G.R. (1998). EIR1,

a root-specific protein involved in auxin transport, is required for gravitropism in *Arabidopsis thaliana*. Genes Dev. **12,** 2175–2187.

Madden, K., and Snyder, M. (1998). Cell polarity and morphogenesis in budding yeast. Annu. Rev. Microbiol. **52,** 687–744.

Migliaccio, F., and Piconese, S. (2001). Spiralisations and tropisms in *Arabidopsis* roots. Trends Plant Sci. **6,** 561–565.

Müller, A., Guan, C., Gälweiler, L., Tänzler, P., Huijser, P., Marchant, A., Parry, G., Bennett, M., Wisman, E., and Palme, K. (1998). *AtPIN2* defines a locus of *Arabidopsis* for root gravitropism control. EMBO J. **17,** 6903–6911.

Nardini, M., and Dijkstra, B.W. (1999). α/β Hydrolase fold enzymes: The family keeps growing. Curr. Opin. Struct. Biol. **9,** 732–737.

Okada, K., and Shimura, Y. (1990). Reversible root tip rotation in *Arabidopsis* seedlings induced by obstacle-touching stimulus. Science **250,** 274–276.

Okada, K., and Shimura, Y. (1994). Modulation of root growth by physical stimuli. In Arabidopsis, E.M. Meyerowitz and C.R. Somerville, eds (Cold Spring Harbor, NY: Cold Spring Harbor Laboratory Press), pp. 665–684.

Oyama, T., Shimura, Y., and Okada, K. (1997). The *Arabidopsis HY5* gene encodes a bZIP protein that regulates stimulus-induced development of root and hypocotyl. Genes Dev. **11,** 2983–2995.

Park, H.O., Bi, E., Pringle, J.R., and Herskowitz, I. (1997). Two active states of the Ras-related Bud1/Rsr1 protein bind to different effectors to determine yeast cell polarity. Proc. Natl. Acad. Sci. USA **94,** 4463–4468.

Parmentier, M.L., Woods, D., Greig, S., Phan, P.G., Radovic, A., Bryant, P., and O'Kane, C.J. (2000). Rapsynoid/partner of inscuteable controls asymmetric division of larval neuroblasts in *Drosophila.* J. Neurosci. **20,** RC84.

Rutherford, R., Gallois, P., and Masson, P.H. (1998). Mutations in *Arabidopsis thaliana* genes involved in the tryptophan biosynthesis pathway affect root waving on tilted agar surfaces. Plant J. **16,** 145–154.

Sakai, T., Wada, T., Ishiguro, S., and Okada, K. (2000). RPT2: A signal transducer of the phototropic response in Arabidopsis. Plant Cell **12,** 225–236.

Sakakibara, H., Kawabara, S., Takahashi, H., Hase, T., and Sugiyama, T. (1992). Molecular cloning of the family of glutamine synthetase genes from maize: Expression of genes for glutamate synthetase and ferredoxin-dependent glutamate synthase in photosynthetic and non-photosynthetic tissues. Plant Cell Physiol. **33,** 49–58.

Sedbrook, J.C., Ehrhardt, D.W., Fisher, S.E., Scheible, W.R., and Somerville, C.R. (2004). The Arabidopsis *SKU6*/*SPIRAL1* gene encodes a plus end-localized microtubule-interacting protein involved in directional cell expansion. Plant Cell **16,** 1506–1520.

Sugimoto, K., Williamson, R.E., and Wasteneys, G.O. (2000). New techniques enable comparative analysis of microtubule orientation, wall texture, and growth rate in intact roots of Arabidopsis. Plant Physiol. **124,** 1493–1506.

Takahashi, N., Goto, N., Okada, K., and Takahashi, H. (2002). Hydrotropism in abscisic acid, wavy, and gravitropic mutants of *Arabidopsis thaliana*. Planta **216,** 203–211.

Thitamadee, S., Tuchihara, K., and Hashimoto, T. (2002). Microtubule basis for left-handed helical growth in *Arabidopsis*. Nature **417,** 193–196.

Whittington, A.T., Vugrek, O., Wei, K.J., Hasenbein, N.G., Sugimoto, K., Rashbrooke, M.C., and Wasteneys, G.O. (2001). MOR1 is essential for organizing cortical microtubules in plants. Nature **411,** 610–613.